# Performance of a SOA-MZI wavelength converter for label swapping using combined FSK/IM modulation format

Available online at www.sciencedirect.com
SCIENCE DIRECT®
Optical Fiber Technology 10 (2004) 31–49
Optical Fiber Technology
www.elsevier.com/locate/yofte

Invited paper

# Performance of a SOA-MZI wavelength converter for label swapping using combined FSK/IM modulation format

I. Tafur Monroy,[a,*] E.J.M. Verdurmen,[a] S. Sulur,[a] A.M.J. Koonen,[a] H. de Waardt,[a] G.D. Khoe,[a] N. Chi,[b] P.V. Holm-Nielsen,[b] J. Zhang,[b] and C. Peucheret [b]

[a] *Eindhoven University of Technology, Eindhoven, The Netherlands*
[b] *COM, Technical University of Denmark, DK-2800 Kgs. Lyngby, Denmark*

Received 24 March 2003; revised 19 May 2003

**Abstract**

This paper presents a theoretical and experimental assessment of the performance of a wavelength converter based on semiconductor optical amplifiers (SOA) in a MZI configuration for optical label swapping. The optical labeling of the signal is based on an FSK/IM combined modulation format for the header/payload, respectively. Experimental results are presented for a signaling scheme with payload data at 10 Gbit/s and an FSK label at 312 Mbit/s. Simulation results and measurements of the chirp properties of converted signals operating at data rates of 2.5 and 10 Gbit/s are presented. Conclusions and design guidelines are presented regarding the implications of the wavelength converter performance on the quality of the label and payload signals for fast packet/burst forwarding in optically labeled switched networks.


*Keywords:* Optical networks; Frequency chirp; Label swapping; Wavelength converter; Packet switching; Burst switching; WDM; IP-over-WDM

* Corresponding author.
*E-mail address:* i.tafur@tue.nl (I.T. Monroy).

1068-5200/$ – see front matter 
doi:10.1016/j.yofte.2003.08.002

## 1. Introduction

Internet protocol (IP) traffic is expected to be the dominant traffic type in future telecommunication networks. Labeled optical packet/burst switched (LOBS) networks are considered a promising solution for fast, flexible and reliable forwarding of IP bursts/packets across optical wavelength division multiplexing (WDM) transport networks [1–5]. Moreover, LOBS are compatible with the general multi-protocol label switching (GMPLS) control mechanism [6]. In a LOBS network, bursts of data are composed by assembling several IP packets in the ingress LOBS nodes according to their destination or class of service. To each burst a label, of a short, fixed length, is assigned and used by the core nodes to forward the packet through the network. Therefore, IP/GMPLS is a low latency, low overhead routing technique that simplifies packet forwarding and enables scaling to terabit rates.

Several techniques have been proposed to label optical packets or burst of packets. One of those is the so-called serial-bit technique, where the label precedes the payload by some time guard [7]. A major disadvantage of this technique when used in LOBS is that the label and payload information are closely coupled requiring time synchronization for label delineation and extraction, and reinsertion of a new label. Another technique is to multiplex the label information by using, for instance, a subcarrier multiplexing (SCM) scheme where labeling information is carried on subcarrier frequency along with the payload data [8]. Although this out-of-band technique decouples payload and label information, it requires a broad spectrum and may suffer from performance degradation due to crosstalk and dispersion. Furthermore, the scalability of the SCM approach to high bit-rate operation may be a hurdle. To lessen the above-mentioned drawbacks, the orthogonal modulation format has been proposed to label optical packets/burst [9,10]. This technique has a compact spectrum and is scalable to high bit-rates. The proposed orthogonal modulation formats are intensity modulation (IM) for the payload and frequency shift keying (FSK) for the label. This IM/FSK modulation scheme is well suited for label erasing and rewriting in a core node composed of a semiconductor optical amplifier Mach–Zehnder interferometer (SOA-MZI) wavelength converter. Moreover, the use of a SOA-MZI structure offers the possibility for integration of a label swapping node in a single photonic circuit. One relevant issue to the performance of the SOA-MZI based label swapping is its chirp performance. In gigabits-per second long-distance direct detection optical telecommunication systems the presence of wavelength chirp may limit the transmission distance and the bit rate. In the proposed FSK/IM labeling scheme, it also may impair the detection of the FSK label information, in particular, if the chirp introduced by the label swapping process is larger than the frequency deviation between the two frequency tones of the FSK signal. In this paper, we present an assessment of the performance of a SOA-MZI based label swapper node and its impact on the quality of an FSK/IM signal. Both simulation results and measurements are presented with emphasis on the chirp performance. This paper is organized as follows. In Section 2, the proposed label swapping scheme together with the label swapping node architecture based on a SOA-MZI wavelength converter is presented. Simulation results of the performance of the FSK/IM modulation scheme are presented in Section 3. In Section 4, experimental results are presented for the performance of a commercially available SOA-MZI converter. In Section 5, we discuss our results and present guidelines for the

design of label swapping nodes supporting IM/FSK modulation format for labeling of IP burst/packets. Finally, in Section 6, summary conclusions are drawn.

## 2. FSK/IM labeling scheme and SOA-MZI wavelength converter based label swapping node

### 2.1. FSK/IM combined modulation scheme

The labeling process of the optical signal is illustrated in Fig. 1. The high-speed payload data is transmitted using intensity modulation, while the label data is conveyed on the same optical carrier by FSK modulation. At the receiver end the payload information can be detected by a simple direct detection scheme. Provided the FSK tone spacing is sufficiently large (e.g., a few tens of GHz), a direct detection scheme precoded by an optical bandpass filter can also be used for detection of the label. Such an optically labeled signal has a compact spectrum. The feasibility of combined intensity modulation and angle modulation has been shown in an experimental WDM network employing a coherent detection scheme [11].

### 2.2. SOA-MZI wavelength converter label swapping node

Figure 2 shows the schematic diagram of a label-swapping node incorporating a SOA-MZI wavelength converter. A small part of the incoming optical power is fed to the label processing circuit. The label is detected and, with a look-up table operation, a new label is defined. The new wavelength label is set by a tunable laser diode, and the incoming intensity-modulated payload data are transferred to this new wavelength by means of an interferometric wavelength converter based on cross-phase modulation in a Mach–Zehnder interferometer (MZI) structure with semiconductor optical amplifiers (SOAs). In the wavelength conversion process, the old FSK information is erased while the payload data is copied onto the new wavelength. The new FSK label is inserted by frequency detuning

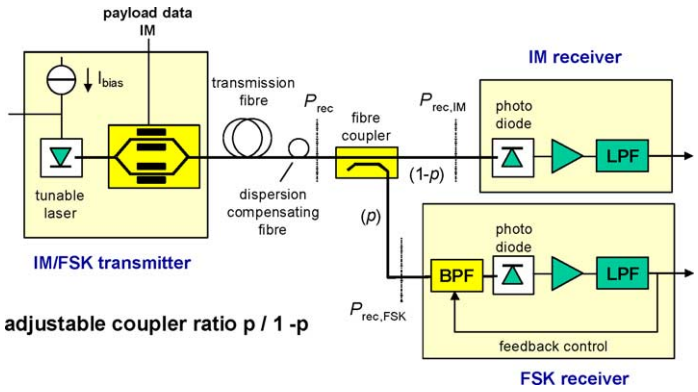


Fig. 1. Schematic diagram of a FSK/IM combined modulation scheme.

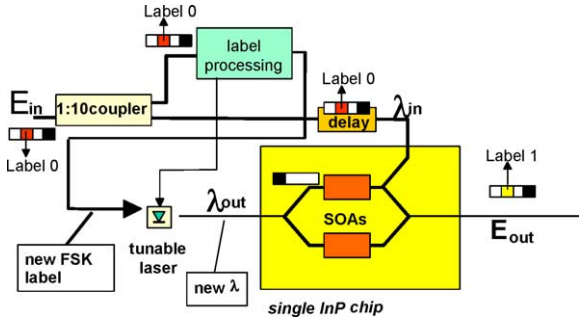


Fig. 2. Schematic diagram for orthogonal FSK/IM labeling in an all optical label swapping node (AOLS) with a SOA-MZI based wavelength converter.

of the incorporated tunable laser. In this way the label swapping is simplified and in the meantime the wavelength conversion functionality can be used for routing purposes and contention resolution. As an alternative to FSK labeling, DPSK labeling is also possible. However, it has been shown that DPSK imposes rigorous requirements on the value of the linewidth parameter of the tunable laser diode [12].

## 3. Simulation results

### *3.1. Combined modulation format FSK/IM*

In order to assess the performance of the combined modulation format, we simulated a transmission link employing a simple direct detection scheme for both FSK and IM. The sample rate used in this simulation is 160 GHz. A Fabry–Perot optical filter is used as bandpass filter for direct detection of FSK at the receiver (see Fig. 1). The simulations assume a $2^{23}$–1 PRBS pattern for the payload data at 10 Gbit/s and a $2^{7}$–1 PRBS pattern for the label signal at 155 Mbit/s. The frequency detuning in the case of FSK is equal to 20 GHz and a laser linewidth of 100 MHz (this relative large value is used to emulate a worst case) and a residual intensity modulation of 0.46 dB are assumed. Of crucial importance in the proposed combined modulation format is the payload extinction ratio. For example, a large extinction ratio is favorable for the IM receiver sensitivity while it is detrimental for the FSK receiver sensitivity, as a FSK bit, imposed on the frequency of several ("zeros" and "ones") IM symbols, should contain sufficient optical power for proper detection. An optimal IM extinction ratio should be obtained in such a way that both the payload and label data can be correctly detected. Hereafter, we define the receiver sensitivity for the IM and the FSK receiver as the average received power to achieve a bit error rate (BER) of $10^{-9}$ and $10^{-12}$, respectively. Figure 3 displays the receiver sensitivity for IM and FSK versus the IM extinction ratio for transmission over a typical standard single mode fiber (SMF) with dispersion of 16 ps/nm/km. An optimum IM extinction ratio for the combined IM/FSK format was found to be around 7 or 8 dB.

As we can see from Fig. 3, the FSK/IM transmission distance is limited to approximately 15 km by fiber dispersion. This is a result of the spectrum spreading between

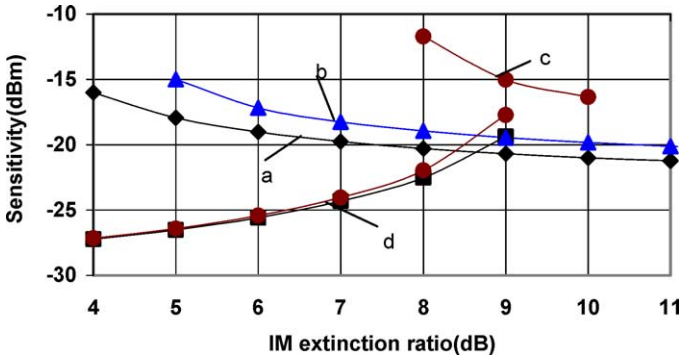


Fig. 3. Receiver sensitivity (IM at BER of $10^{-9}$ and FSK at BER $10^{-12}$) against payload extinction ratio for various SMF lengths. $a = 10$ km, $b = 15$ km, $c = 18$ km for IM and $d = 10$, 15, 18 km for FSK.

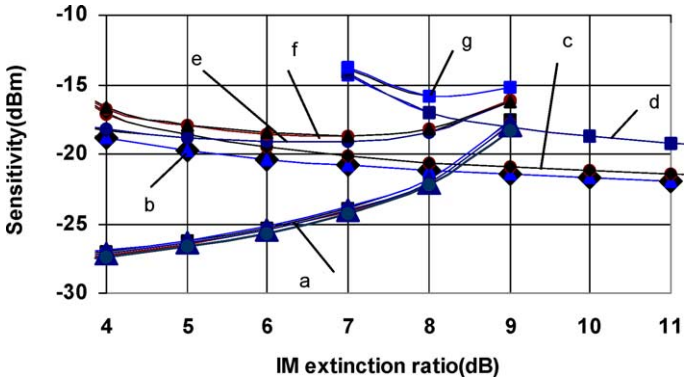


Fig. 4. Sensitivity (IM at BER of $10^{-9}$ and FSK at BER $10^{-12}$) as a function of IM extinction ratio at FSK frequency deviation of 20 GHz for several values of laser linewidth and the residual amplitude modulation after a 60 km SMF dispersion compensated link ($a$ = FSK: 50, 100 MHz; 0, 0.46, and 0.97 dB, $b$ = IM: 50, 100 MHz; 0 dB, $c$ = IM: 50, 100 MHz; 0.46 dB, $d$ = IM: 50, 100 MHz; 0.97 dB, $e$ = overall: 50, 100 MHz; 0 dB, $f$ = overall: 50, 100 MHz; 0.46 dB, $g$ = overall: 50, 100 MHz; 0.97 dB).

the FSK tones spaced at 20 GHz, which however can be overcome by using dispersion compensating fiber (DCF). In Fig. 4 we show the receiver sensitivity as a function of the payload extinction ratio for both IM payload and FSK label when DCF is employed to compensate for the dispersion of SMF. The dispersion at 1553.6 nm of the SMF and the DCF is 16.9 and $-100$ ps/nm/km, respectively. The dispersion slope of the SMF is 0.0578 ps/nm$^2$/km, and $-0.23$ ps/nm$^2$/km for the DCF. We used 60 km SMF and 9.6 km DCF for complete dispersion compensation. The impact of laser linewidth and residual amplitude modulation to the IM and FSK receiver sensitivities are also shown in Fig. 4 where we can see that the performance of the IM/FSK combined modulation format is robust to large values of the laser linewidth in the order of 100 MHz in a transmission link of 60 km of SMF with full dispersion compensation.

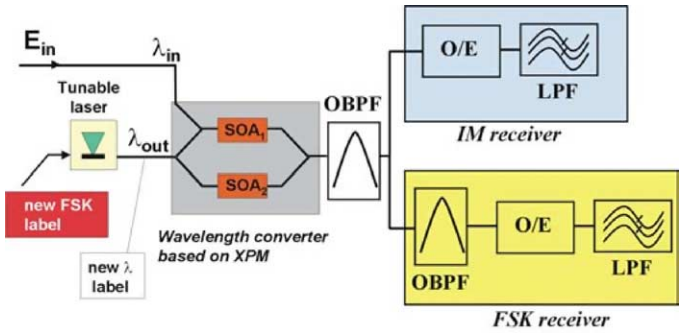


Fig. 5. Simulation scheme for the performance of the SOA-MZI based wavelength converter supporting FSK/IM modulation format. OBPF: optical bandpass filter, LPF: low pass filter.

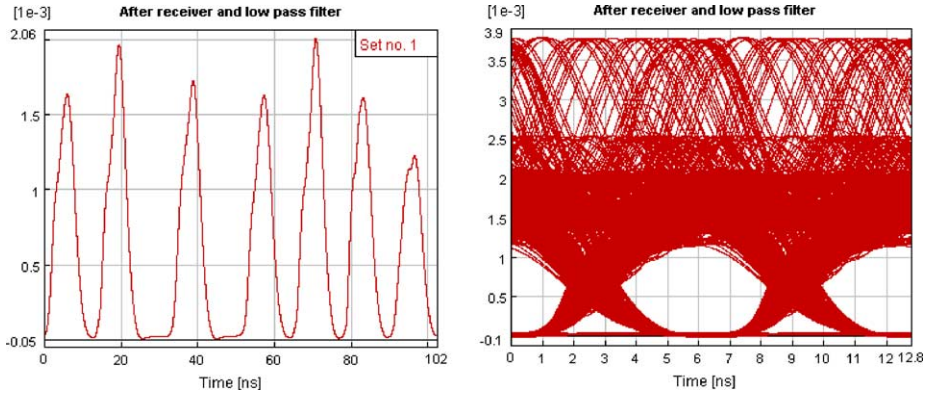


Fig. 6. Simulated FSK signal bit pattern (left) and eye diagram (right); the unit of the vertical axes is mW.

### 3.2. SOA-MZI based wavelength converter

To investigate the performance of the SOA-MZI wavelength converter based on Cross Phase Modulation (XPM), we have performed simulations in VPI TransmissionMaker software.[1] The schematic diagram of the simulations is shown in Fig. 5.

The simulated system operates at 10 Gbit/s for the payload and 155 Mbit/s for the label with a frequency deviation of 20 GHz. For the simulation we used a probe power of 0 dB m, and a laser linewidth of 10 MHz for the probe as well as pump signal. The converted signal is filtered by an OBPF, with a bandwidth of 40 GHz, to filter out the old wavelength. The OBPF for the FSK receiver has a bandwidth of 4 GHz, in order to be able to select one of the frequency tones. The IM input signal had a modulation index $m = 0.8$, which corresponds to an extinction ratio of 6 dB. An example of the simulated IM/FSK signal at the transmitter output (signal $E_{\text{in}}$ in Fig. 5) is shown in Fig. 6.

[1] Software tool of VPIsystems (www.vpisystems.com).

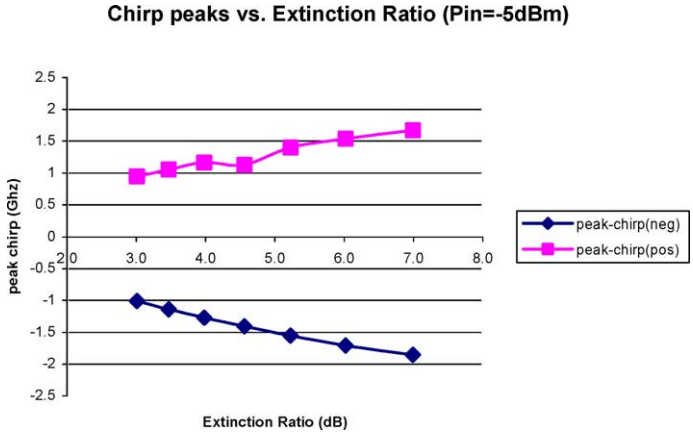


Fig. 7. Simulation results for the chirp peaks (GHz) versus the extinction ratio (dB) of the input signal.

We can clearly see the pattern dependence of the FSK signal in Fig. 6. This effect has also been observed experimentally, as shown in Fig. 15. The variation of the one-level of the label is due to the payload bit stream at 10 Gbit/s. During the transmission of one label bit there are 64 payload bits sent on the same optical carrier. Depending on the number of "*ones*" in the 64 bit sequence of the payload, the power level is higher or lower for the simultaneously transmitted FSK-bit. This power dependence of a binary "*one*" can also be clearly seen in the eye-diagram in Fig. 6. However the eye-opening is still clear, which means that the signal can be received error free. However an additional performance penalty is expected due to the fluctuation of the "*one*" level.

### *3.3. Chirp performance*

The presence of frequency chirp may degrade the performance of the IM/FSK signal. By measuring the time-resolved chirp, detailed and reliable information about the wavelength converter dynamics can be obtained. This is in contrast to measuring the time-averaged chirp, e.g., on a spectrum analyzer. The experimental results will be shown in Section 4.3 while in this section the results of the simulations are presented. The simulated chirp is shown in Fig. 7 for several values of the extinction ratio of the input signal. The simulated chirp peaks are between 1 and 2 GHz, and the peak-to-peak values are between 2 and 4 GHz. A difference between the simulations and the actual experimental work is the polarization independence of the simulation models.

## 4. Experimental assessment

### *4.1. Experimental setup*

The experimental results were obtained using an integrated all-active three-port SOA-MZI wavelength converter from Alcatel, shown in Fig. 8. The wavelength converter can be

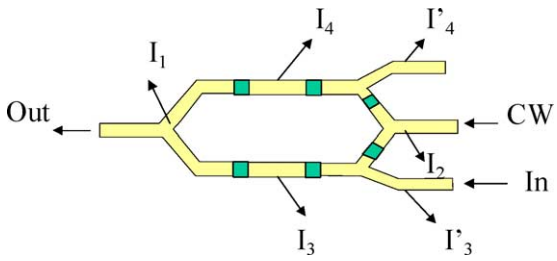


Fig. 8. A schematic of the SOA-MZI wavelength converter from Alcatel, in co-propagating operation mode. The set of driver currents are also given.

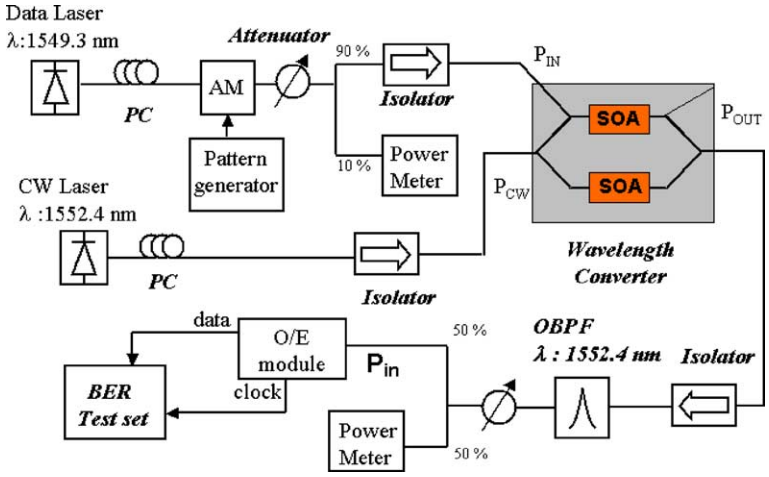


Fig. 9. Experimental setup for measuring the BER performance of the SOA-MZI wavelength converter.

operated in non-inverting and inverting mode. In both operation modes the receiver sensitivity and the dynamic range are compared. The experimental setup is shown in Fig. 9. The pump is intensity modulated at 10 Gbit/s. The wavelength of the pump signal is 1549.3 nm. The probe is a continuous wave (CW) signal with $\lambda = 1552.4$ nm. This corresponds with the peak transmission of the OBPF (bandwidth is 0.73 nm) at the output of the wavelength converter. For co-propagating signals, the currents applied to the wavelength converter are $I_1 = 100$, $I_2 = 40$, $I_3 = 350$, $I_3' = 35$, $I_4 = 205$, and $I_4' = 25$ mA for the inverting operation. For the non-inverting operation we used $I_1 = 120$, $I_2 = 50$, $I_3 = 250$, $I_3' = 30$, $I_4 = 70$, and $I_4' = 25$ mA.

### 4.2. Dynamic range and pattern dependence

The power penalty (the increase in optical received power to obtain a BER of $10^{-9}$, compared to the back-to-back configuration) for the wavelength conversion is measured at 2.5 and at 10 Gbit/s. This is performed for non-inverting and inverting co-propagating operation mode. The penalty at 2.5 Gbit/s is 1 dB for the inverting operation and 1.5 dB for

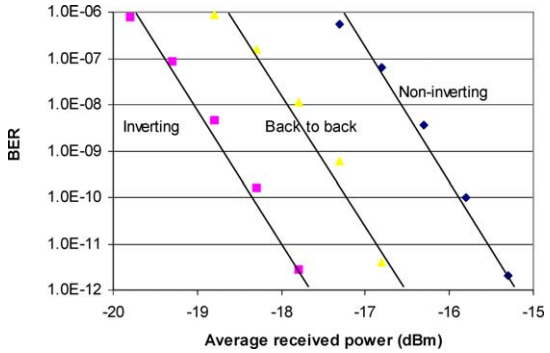


Fig. 10. BER curves for inverting, non-inverting operation and the back-to-back system at 10 Gbit/s.

the non-inverting operation. The counter-propagating operation is not very attractive due to the counter-directional coupling that causes pattern-dependent timing jitter, which limits the cascadeability. Moreover, the conversion speed is limited by a modulation bandwidth, which is inherently lower than for co-directional coupling [13–15]. The fastest achieved conversion for counter-propagating operation mode was measured for a non-inverting current setting at 2.5 Gbit/s. By optimizing the system the penalty is minimized to 1 dB. For wavelength conversion at 10 Gbit/s the power penalty is only measured for co-propagating conversion. The BER curves for inverting, non-inverting operation and the back-to-back system are shown in Fig. 10. For non-inverting operation we found a 1 dB power penalty, but for inverting operation we found a regenerative effect of 1 dB. The 1-dB sensitivity improvement for inverting operation shows the regenerative effect of the MZI wavelength converter based on XPM and can be explained by the extinction ratio improvement. However, for label swapping of a combined FSK/IM modulated signal, it is desirable that the extinction ration is kept constant for proper operation of the FSK receiver. For non-inverting operation the 1-dB penalty is likely to be caused by the lower extinction ratio of the converted signal.

One of the most important parameters to characterize is the dynamic range of the wavelength converter. The data signals in an optical network do not always have the same power level when they reach an AOLS node. The 3-dB dynamic range for 2.5 Gbit/s operation is largest for the non-inverting co-propagating mode. The results for non-inverting and inverting operation are respectively 3.9 and 2.6 dB for the 3-dB dynamic range. Inverting operation is still preferable above non-inverting, due to its larger regenerative effect. The conversion speed of the present device for the counter-propagation mode is measured to be far slower compared to the co-propagating operation, what is generally the case for SOA-MZI wavelength converters [15]. Therefore, the measurement at 10 Gbit/s is only performed in co-propagating operation mode. The result of the dynamic range measurement at 10 Gbit/s inverting operation is shown in Fig. 11. The range in which the power penalty is smaller than 2 dB compared to the back-to-back system is 3.7 dB for inverting operation and 1.7 dB for non-inverting operation. We can conclude that for the given drive currents of the different SOA's, the co-propagating inverting operation has the best

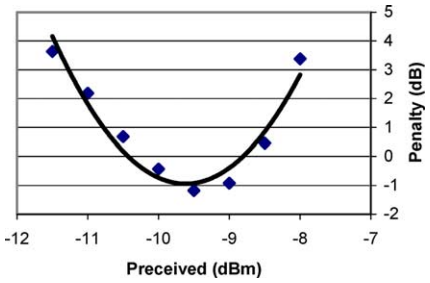


Fig. 11. Dynamic range of the SOA-MZI wavelength converter in the inverting co-propagating operating regime at 10 Gbit/s.

performance. To accommodate larger input power variations some form of automatic gain control will be required.

### *4.3. Chirp performance*

Interferometric wavelength converters based on XPM reduce the chirp problem that exists in Cross Gain Modulation (XGM) based converters. Namely, the height of the chirp peak is much lower for the XPM based converters. A detailed experimental study of the chirp performance of XPM is given in [13]. For a combined IM/FSK modulation format, it is of great importance to find the value of the chirp peak to determine the influence on the orthogonal modulation format FSK. The chirp measurement method is based on a Fabry–Perot (FP) interferometer as frequency discriminator [16]. The chirp analysis block diagram is shown in Fig. 12.

The EDFA is used as a pre-amplifier to compensate for the high losses in the FP. For the tuning of the filter a battery voltage is used, to avoid fluctuations of the peak-wavelength of the FP. The signal is split with a 90–10 coupler of which the 10% port is connected to the power meter to tune the FWHM point of the FP transfer function, and the 90% port is used to record the bit pattern at that FWHM point with an optical sampling scope. The experiments show us that the magnitude of the chirp is smaller than 5 GHz peak-to-peak, and the sign of the chirp depends on the operation mode of the wavelength converter. For non-inverting operation, the red and blue chirp peaks occur respectively on the rising and falling edges of the output signal. For inverting operation opposite behavior is observed. This is in accordance with previous theoretical studies [13]. An example of the result of the chirp measurement is shown in Fig. 13.

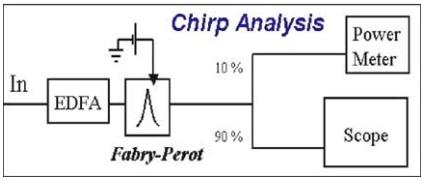


Fig. 12. Schematic of the chirp analysis setup.

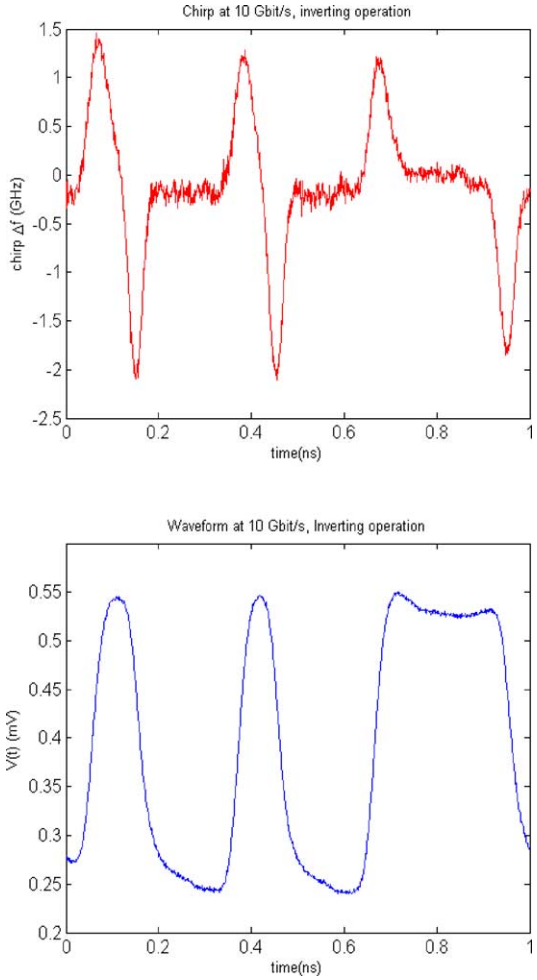


Fig. 13. Time-resolved chirp (top) and corresponding waveform (bottom) at 10 Gbit/s inverting co-propagating operation.

Chirping results in a broadening of the signal spectrum, and if this broadening is too large the FSK modulated label will be influenced. The chirp measurements were carried out for 2.5 Gbit/s as well as for 10 Gbit/s. No substantial difference in peak-to-peak chirp was observed. To determine the influence of the chirp on the FSK modulated label information, we compared the chirp measurements with the FSK frequency spacing (20 GHz). There is no degradation of the FSK signal as long as the chirp falls within the bandwidth of one of the optical filters used for direct detection of the FSK-tone. In the experiments we observed no chirp peaks higher than 3 GHz and the peak-to-peak chirp varied between 3.5 and 5 GHz. This means that with a frequency tone spacing of 20 GHz, the FSK signal performance will not be degraded by the chirp. The power in the chirp peaks is calculated for several different pulse patterns and operating modes of the wavelength converter. The

percentage of the power of the light wave with chirp peaks larger than |0.5| GHz is between 30–50%. For chirp peaks larger than |1.0| GHz this percentage is in the range of 10–30%, while it is only 0–8% for chirp peaks large than |2.0| GHz. Chirp measurements were also performed for a 2.5 Gbit/s data stream generated by direct current modulation of a DFB laser instead of using a low-chirp external modulator. No substantial difference for the chirp behavior was observed between these two cases. This is in accordance to earlier published results for a similar SOA-MZI device [17].

### *4.4. FSK/IM label swapping*

The performance of the SOA-MZI based wavelength converter was experimentally studied for a payload rate at 10 Gbit/s and a FSK label rate at 312 Mbit/s. The experimental setup for the label erasure and label insertion is depicted in Fig. 14. The optical FSK modulation can be achieved simply by directly modulating the electrical current of a DFB laser diode at 1549.3 nm. However, the drive current variation always results in a simultaneous intensity modulation of the emitted light. Obviously, such a residual intensity modulation has a detrimental effect on the intensity-modulated payload. To remove the intensity variation of the laser's output, the inverse electrical data is injected into the integrated electro-absorption modulator (EAM) with appropriate time delay and modulation voltage. In this way, a constant amplitude optical FSK signal is generated.

The payload information at 10 Gbit/s is added by a subsequent Mach–Zehnder modulator, thus producing an optically FSK labeled signal. This signal is then injected into the SOA-MZI with a CW light at 1554.1 nm, which is generated by a tunable external cavity laser (ECL). At the output of the SOA, an arrayed waveguide grating (AWG) is used to filter out the converted signal. Because of the wavelength conversion in the SOA-MZI, the 10 Gbit/s IM payload is copied onto the CW light while the FSK label will not be converted to the new wavelength. Hence the label erasure is accomplished. The output payload eye diagram after label removal is shown in Fig. 15a. For an input payload with extinction ratio of 4.5 dB, the output signal has an extinction ratio of 12.9 dB, resulting in an increase in receiver sensitivity of 2 dB compared to back-to-back case, clearly demonstrating the 2R regeneration due to the SOA-MZI. In Figs. 15b and 15c a measured bit-pattern of the detected FSK label signal and it's the corresponding eye diagram are shown. We can clearly see the pattern dependence introduced by the 10 Gbit/s IM payload. However, the eye diagram remains open and the FSK label can be properly recovered. Figure 16 shows the dependence of the BER on the received power for a back-to back configuration of the FSK/IM combined modulation format. We can see that the receiver sensitivity at a BER of $10^{-9}$ is $-32.6$ and $-24.2$ dB m, for the FSK label and IM payload, respectively (curves marked with (■), and (▼), respectively).

A label insertion scheme was realized using a FSK modulated signal instead of a CW signal at the SOA-MZI converter. The signal output of the SOA-MZI device is then the original payload data, converted to the FSK signal wavelength, with the superimposed FSK label modulation. After splitting the signal for FSK and IM detection, the BER was measured as a function of the average received power. The results are presented in Fig. 16. As we can see the receiver sensitivity at a BER of $10^{-9}$ is $-31$ and $-23.5$ dB m, for the label and payload, respectively (curves marked (□) and (▽), respectively). We observe

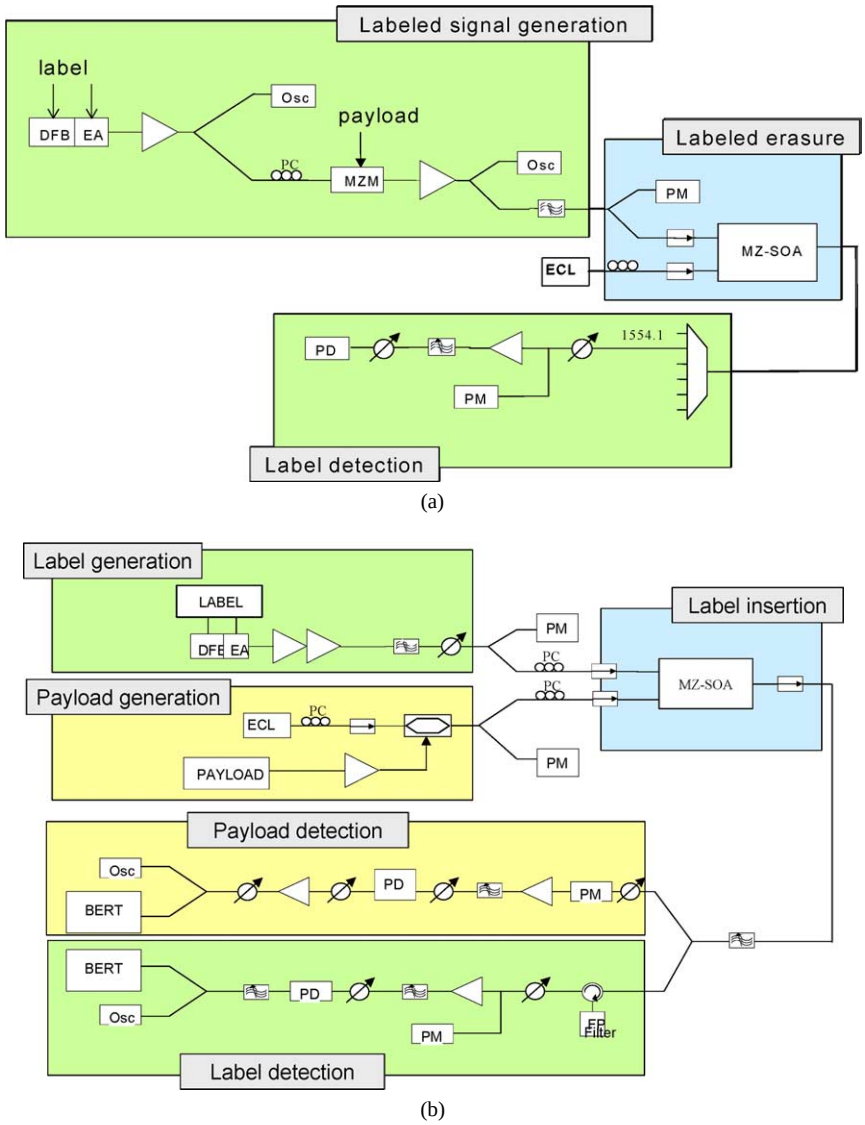


Fig. 14. Experimental setups for FSK label (a) erasure and (b) insertion using a SOA-MZI wavelength converter. ECL: external cavity laser, PM: power meter, PC: polarization controller.

that no substantial degradation of the receiver sensitivity takes place in the label insertion process. In fact, the SOA-MZI has a regenerative character. However, for a proper detection of the FSK signal, a certain power level in the "zeros" bit should be present. The extinction ratio of the input signal was measured to be 5.1 dB and an extinction ratio of 4 dB was observed at the output of the SOA-MZI. The error free detection of the FSK data experimentally demonstrates that the chirp introduced by the SOA-MZI wavelength converter has no detrimental influence on the FSK detection.

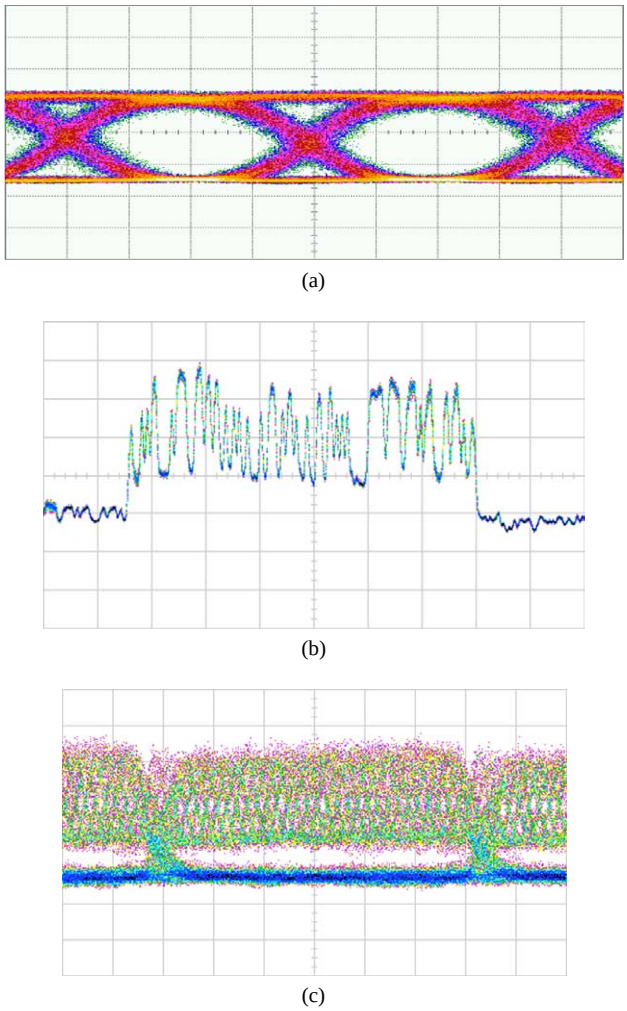

Fig. 15. (a) Payload eye diagram after label removal, (b) measured pulse pattern, and (c) eye pattern of detected FSK modulation at 312 Mbit/s, superimposed orthogonally to a 10 Gbit/s IM pattern.

### *4.5. BER measurements*

To examine the erasure capability of the label data after wavelength conversion in the SOA-MZI device, a combined FSK/IM modulates signal was used as the signal input while a CW signal was used for the new wavelength signal, as shown in Fig. 14a. No FSK modulation was observed at the new converted wavelength while the IM was detected error free. A plot of the BER as a function of the input power for the payload signal is shown in Fig. 16 (curve marked (◆)), to be compared with the back-to-back result. This same IM signal was used as a probe signal onto which a new FSK label is superimposed by cross

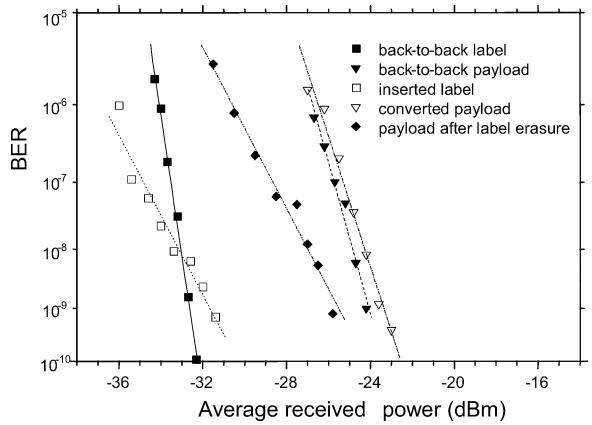


Fig. 16. BER versus receiver input power for the IM payload and the FSK label. (a) Label in the back-to-back configuration (■), (b) payload back-to-back (▼), (c) payload after wavelength conversion and FSK label insertion (▽), (d) inserted FSK label (□), and (e) payload after label erasure (◆).

absorption modulation (XAM) in EAM. This experiment is presented in detail in the next section.

### *4.6. FSK label swapping*

The complete operation of label swapping (i.e., label erasure and insertion of a new FSK label) can be performed with the SOA-MZI under study provided a second FSK signal is available at a different wavelength than the old FSK label to be erased. This second FSK signal is then used instead of the CW input into the SOA-MZI wavelength converter. Although, a counter-propagation mode of operation could be used, the SOA-MZI device under study shows insufficient performance for data rates above 5 Gbit/s, as discussed in Section 4.2. To study the chirp and linewidth properties of the IM converted signal after FSK erasure, and to assess its suitability for FSK label re-insertion, the experimental setup shown in Fig. 17 was used. The output of the SOA-MZI wavelength converter was fed into an optical add drop multiplexer (OADM) to filter out the old wavelength signal. Then the signal is amplified and fed into an EAM where FSK label insertion took place by XAM using an FSK modulated pump signal. Experiments using a FSK pump signal at the 'CW' port of the SOA-MZI (see Fig. 17) are under study and their results will be published elsewhere.

The results for the BER measurements for the FSK and IM signals after a complete label swapping stage are shown in Fig. 18. We can compare these results with the back-to-back measurements presented in Fig. 16. As we can see, there is no substantial power penalty for both signals; instead we can observe a small regenerative effect of about 0.5 dB of receiver sensitivity enhancement. We may observe from the optical spectrum (see Fig. 19) that there is no substantial spectrum broadening due to the label swapping. The chirp introduced by the SOA-MZI has therefore no effect on the performance, as confirmed by the error free detection of the FSK signal. This is in accordance with the previous chirp measurements and simulations results presented in Sections 3.3 and 4.3.

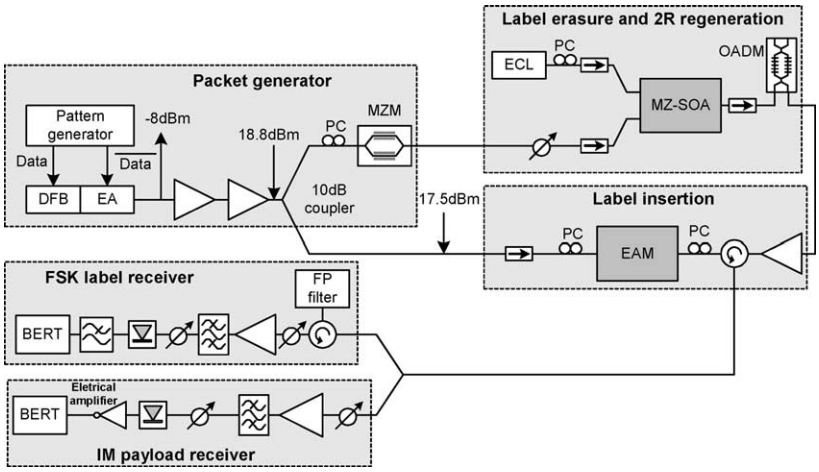


Fig. 17. Setup for a complete label swapping of FSK/IM labeled signal. OADM: optical add drop multiplexer.

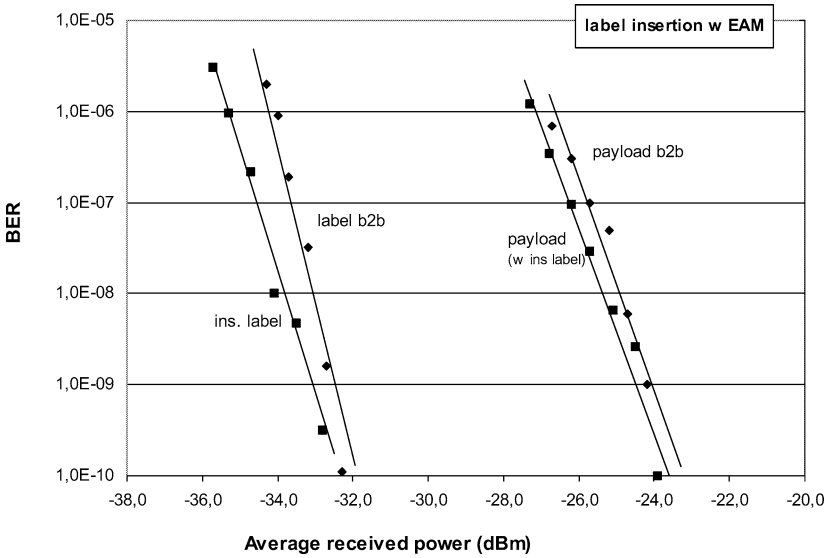


Fig. 18. BER versus input power for a FSK/IM combined modulation scheme after a complete label swapping stage. The results are to be compared with the back-to-back curves of Fig. 16.

## 5. Discussion of results

### *5.1. FSK/IM modulation format*

The extinction ratio of the IM is a crucial design parameter for a combined FSK/IM system. Namely, there should be enough optical power in the IM "zero" binary symbols so that the FSK data still can be recovered. Experimentally, it has been shown that an

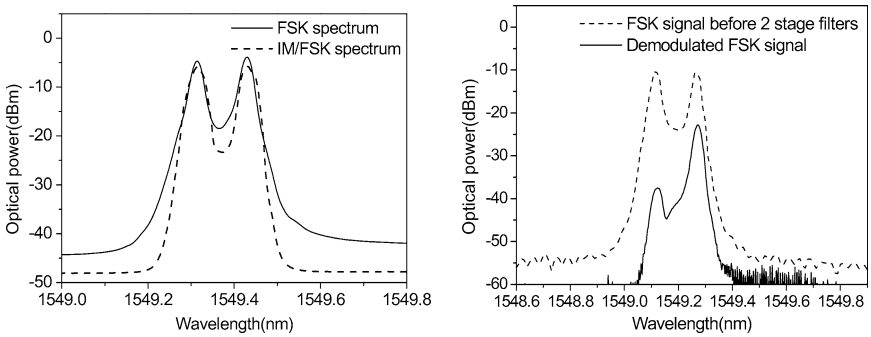


Fig. 19. (a) Optical spectra of the pure FSK signal and IM/FSK signal. (b) Received IM/FSK signal at the output of the frequency discriminator.

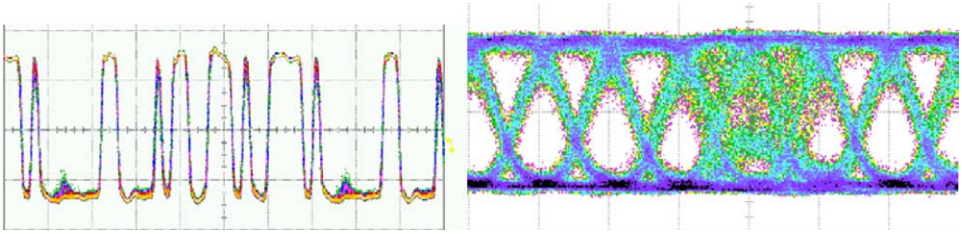

Fig. 20. Example of a detected 10 Gbit/s IM bit pattern and eye diagram when the IM and the FSK bit at 312 Mbit/s are not perfectly synchronized.

extinction ratio (ER) of 4–5 dB gives proper performance. Another aspect relevant to the design of the combined modulation format is the synchronization between the FSK bit and the IM bit. Figure 20 shows examples when the FSK and IM bits are not perfectly synchronized. In this case the eye pattern is distorted and errors are detected. This effect is accumulative in the case of label swapping, as therefore the performance degradation may be severe.

### *5.2. Chirp performance*

According to our experiments and simulations, for a system operating at 10 Gbit/s the chirp peaks introduced by the SOA-MZI are limited to a magnitude smaller than |3| GHz. Moreover, the signal power contents of these chirp frequency peaks larger than |2| GHz is less than 8% of the total optical power in a bit-time slot. This indicates that, for instance, FSK modulation with a frequency deviation of 10–20 GHz is feasible. Experiments confirm that this is the case for a 312 Mb/s FSK signal with a frequency deviation of 20 GHz.

### *5.3. FSK label swapping with SOA-MZI converters*

In an optical network, channels arriving from different nodes at a label swapping node may have different power labels. The dynamic range of the SOA-MZI converter has to be large enough to cope with these power differences. The dynamic range of the SOA-MZI device under study is limited to 3 dB, which is in agreement with other results published in the literature [14]. As a consequence, dynamic range extension by using for instance a pre-stage amplification with automatic gain control (AGC) should be implemented. Another aspect of relevance to the performance of the FSK/IM modulation format is that the optimal extinction ratio of the IM signal should be preserved after label swapping to guarantee a good FSK performance.

## 6. Conclusions

Combined FSK/IM modulation format is shown theoretically and experimentally to be a promising technique to label optical signals for deployment in optically labeled burst/packet switched networks. The feasibility of performing FSK label swapping and wavelength conversion in a SOA-MZI wavelength converter is studied both theoretically and experimentally. The results show that a SOA-MZI device can be used to perform the label swapping of FSK/IM labeled signals with no substantial degradation of the signal quality. Measurements of the BER for a IM payload at 10 Gbit/s and a FSK label at 312 Mbit/s show that the chirp properties of the SOA-MZI allow for successful FSK label erasure and insertion of a new FSK label with no observed signal degradation. These results point out that an optical label swapping node can be built using a SOA-MZI based device that is suitable for integration in a photonic circuit. Furthermore, the studied SOA-MZI technology and combined FSK/IM modulation format for optical labeling of signals are scalable to higher bit-rates.

## Acknowledgments

This work was supported by the 5th framework IST-project STOLAS which is partially funded by the European Commission. Contributions of the other STOLAS partners (IMEC Ghent, Lucent, UC Dublin, Hymite, NKT Integration, Telenor) are also gratefully acknowledged. The simulations were performed using the VPI software tool.

## References

[1] D. Colle, S. De Maesschalck, C. Develder, P. Van Heuven, A. Groebbens, J. Cheyns, I. Lievens, M. Pickavet, P. Lagasse, P. Demeester, Data-centric optical networks and their survivability, IEEE J. Sel. Area Comm. 20 (1) (2002) 6–20.

[2] S. Yao, B. Mukherjee, S. Dixit, Advances in photonic packet-switching: An overview, IEEE Commun. Mag. (2000) 84–93.

[3] C. Qiao, M. Yoo, Optical burst switching (OBS)—a new paradigm for an optical internet, Special Issue on WDM Networks, J. High Speed Netw. 8 (1) (1999) 69–84.
[4] J.S. Turner, WDM burst switching for petabit data networks, in: Optical Fiber Communication Conference, Vol. 2, 2000, pp. 47–49.
[5] C. Qiao, Labeled optical burst switching for IP-over-WDM integration, IEEE Commun. Mag. (2000) 104–114.
[6] A. Banerjee, et al., Generalized multiprotocol label switching: An overview of routing and management enhancements, IEEE Commun. Mag. (2001) 144–150.
[7] C. Guillemot, M. Renaud, P. Gambini, et al., Transparent optical packet switching: The European ACTS KEOPS project approach, J. Lightwave Technol. 16 (12) (1998) 2117–2134.
[8] D.J. Blumenthal, B.-E. Olsson, G. Rossi, T.E. Dimmick, L. Rau, M. Masanovic, O. Lavrova, R. Doshi, O. Jerphagnon, J.E. Bowers, V. Kaman, L.A. Coldren, J. Barton, All-optical label swapping networks and technologies, J. Lightwave Technol. 18 (12) (2000) 2058–2075.
[9] T. Koonen, G. Morthier, J. Jennen, H. de Waardt, P. Demeester, Optical packet routing in IP-over-WDM networks deploying two-level optical labeling, in: Proceedings of ECOC'01, Amsterdam, 2001, paper Th.L. 2.1.
[10] E.N. Lallas, N. Skarmoutsos, D. Syvridis, An optical FSK-based label coding technique for the realization of the all-optical label swapping, IEEE Photon. Technol. Lett. 14 (10) (2002) 1472–1474.
[11] M. Hickey, L. Kazovsky, The STARNET coherent WDM computer communication network: Experimental transceiver employing a novel modulation format, J. Lightwave Technol. 12 (5) (1994) 876–884.
[12] A.M.J. Koonen, S. Sulur, I. Tafur Monroy, J.G.L. Jennen, H. de Waardt, Orthogonal optical labeling of packets in IP-over-WDM networks, in: Proceedings of NOC 2002, 7th European Conference on Networks & Optical Communications, Darmstadt, Germany, 2002, pp. 82–89.
[13] H. Lee, H. Yoon, Y. Kom, J. Jeong, Theoretical study of frequency chirping and extinction ratio of wavelength-converted optical signals by XGM and XPM using SOA's, IEEE J. Quant. Electron. 35 (1999) 1213–1219.
[14] T. Durhuus, B. Mikkelsen, C. Joergensen, S.L. Danielsen, K.E. Stubkjaer, All-optical wavelength conversion by semiconductor optical amplifiers, J. Lightwave Technol. 14 (1996) 942–954.
[15] C. Joergensen, et al., All-optical wavelength conversion at bit rates above 10 Gb/s using semiconductor optical amplifiers, IEEE J. Sel. Top. Quant. 3 (5) (1997) 1168–1180.
[16] S. Tammela, H. Ludvigsen, T. Kajava, M. Kaivola, Characterization of the chirp and intensity modulation properties of an SOA-MZI wavelength converter, IEEE Photon. Technol. Lett. 9 (1997) 475–477.
[17] S.-C. Cao, J.C. Cartledge, Characterization of the chirp and intensity modulation properties of an SOA-MZI wavelength converter, J. Lightwave Technol. 20 (4) (2002) 689–695.